Heliyon 10 (2024) e31917

Contents lists available at ScienceDirect

Heliyon

journal homepage: www.cell.com/heliyon

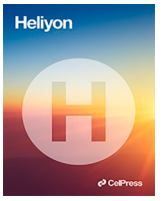

Research article

Profound perturbations are found in the proteome and metabolome in children with obesity after weight loss intervention

Xiaoguang Liu [a,b], Huiguo Wang [a,b], Lin Zhu [a,b,*]

[a] School of Sport and Health, Guangzhou Sport University, Guangzhou, China
[b] Guangdong Provincial Key Laboratory of Physical Activity and Health Promotion, Guangzhou Sport University, Guangzhou, China

ARTICLE INFO

Keywords:
Weight loss
Obese children
Proteome
Metabolome

ABSTRACT

Background and aims: The mechanisms occur in children with obesity after lifestyle intervention remain poorly explained. Here, we investigated the serum proteomes and metabolomes of children with obesity who had undergone 30 days of weight loss intervention.

Methods and results: Serum samples and clinical parameters were collected before and after lifestyle alteration interventions. Proteomic and metabolomic profiling was used to identify the differentially expressed proteins and differentially abundant metabolites in response to weight loss intervention. Lifestyle alteration interventions significantly decreased BMI, waist circumference, hip circumference and body fat, total cholesterol (TC), triglyceride (TG), low-density lipoprotein cholesterol (LDL) and high non-HDL cholesterol, but not TG and high-density lipoprotein cholesterol (HDL), in children with obesity. By comparing the multiomics data, we identified 43 proteins and 165 metabolites that were significantly differentially expressed in children with obesity before and after lifestyle alteration interventions. Using integrated -omics analysis, we obtained 7 KEGG pathways that were organically integrated based on the correlations between differentially expressed proteins (DEPs) and metabolites (DMs). Further interaction analysis identified 7 proteins as candidate DEPs and 9 metabolites as candidate DMs. Interestingly, we found that some of these candidate DEPs and candidate DMs were significantly correlated with clinical parameters.

Conclusion: Our results provide valuable proteome and metabolome data resources for better understanding weight loss-associated responses in children with obesity. In addition, we analyzed the number of significantly differentially expressed proteins and metabolites, shed new light on weight loss pathogenesis in children with obesity, and added potential therapeutic agents for obese children.

1. Introduction

Obesity and overweight are defined as abnormal or excessive accumulation of fat tissue in the body, which may result in an unhealthy body shape and disease. The prevalence of obesity is increasing in children, adolescents and adults worldwide [1]. The World Health Organization (WHO) reported that the prevalence of overweight and obesity significantly increased from 4 % to 18 % in children and adolescents from 1975 to 2016. In addition, there were more than 340 million overweight or obese children in 2016 [2].

* Corresponding author. School of Sport and Health, Guangzhou Sport University, Guangzhou, China.
E-mail address: 11251@gzsport.edu.cn (L. Zhu).

https://doi.org/10.1016/j.heliyon.2024.e31917
Received 25 January 2024; Received in revised form 23 May 2024; Accepted 23 May 2024
Available online 25 May 2024

The incidence of obesity in children increases the risk of additional comorbidities, such as hypertension, dyslipidemia, diabetes, and other cardiovascular diseases, in adulthood [3].

Lifestyle alteration is the first-line approach to the prevention and treatment of obesity and overweight in children and adults [4]. Lifestyle alterations include diet modification and increased physical activity. Ryan et al. [5] found that moderate-intensity exercise and high-intensity exercise interval training improved insulin sensitivity in adults with obesity. Moreover, emerging evidence has demonstrated that exercise intervention can improve body composition in obese and overweight children [6]. Although recent studies have explored the mechanism of weight loss following lifestyle alterations, the mechanism is not fully understood.

Blood acts as a fluid transport for circulating small molecules inside the body. These small molecules in serum are termed the serum metabolome. Cropulence results in a significant disruption of the serum metabolome [7]. In addition, lifestyle alteration-based weight loss interventions significantly change the serum metabolomic signatures in obese or overweight children and adolescents [8]. Proteins perform most biological processes, such as metabolic liaisons of life, and the profound perturbation of the serum metabolome commonly occurs with pathology onset and progression [9]. Studies have found that the levels of numerous proteins are significantly different between normal weight and obese or overweight individuals [10,11]. More critically, numerous proteins have been demonstrated to be differentially transported in the sera of individuals with obesity after weight loss intervention [9].

Research has investigated the proteomics and metabolomics of adipose tissue in obese rabbits that have experienced weight loss [12]. No studies had specifically focused on examining the metabolites, proteomics, and their interactions in children with obesity both prior to and following weight loss interventions. Consequently, the aim of this study is to focus a multiomics approach on the metabolite and proteomics changes in children with obesity following weight loss interventions.

2. Methods and materials

2.1. Ethics and study design

This study was approved by the Ethical Committee of Guangzhou Sport University (No. 2018LCLL-008), and written informed consent was signed by all the children and their parents. The investigation conforms with The Code of Ethics of the World Medical Association. Serum samples from 6 children with obesity were collected before and after weight loss interventions. Metabolome and proteome analyses were performed in this study (Fig. 1).

2.2. Participant inclusion criteria

From June 2022 to August 2022, 6 children with obesity aged 10–14 years were selected from the training camp (Shenzhen, China). Children with obesity were defined as having a body mass index (BMI) that corresponded to the guidelines for obesity. All children were free of heart disease, kidney disease, hepatitis B, and chronic illnesses and had no history of medication.

The children with obesity performed a 30-day weight loss intervention, including diet control and exercise in closed training camps. To ensure effective interventions, dietary intake and exercise training volume and intensity were monitored and recorded. The details of the diet control and exercise intervention were described in a previous study [13].

2.3. Clinical data collection and procedure

The clinical data were collected before and after the weight loss intervention. Height was measured by a standard height meter,

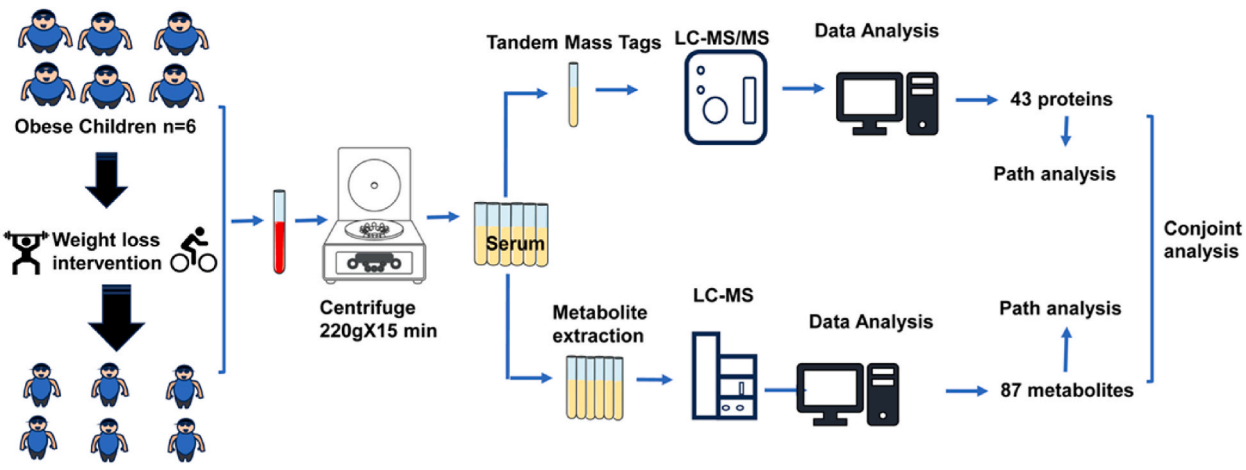

Fig. 1. Study design and blood samples. Overview of serum samples collected from obese children before (n = 6) and after (n = 6) weight loss interventions. The flowchart shows the process of proteomic and metabolomic analysis.

weight was measured by a digital scale, and all measurements were rounded to the nearest 0.1 cm or 0.1 kg. Body mass index (BMI) was determined by weight in kilograms divided by the height in meters squared. Waist and hip circumference were measured by a plastic tape to the nearest 0.1 cm. Body fat was measured by a body composition analyzer (T-SCAN PLUS, Korea).

The concentrations of total cholesterol (TC), triglycerides (TGs), low-density lipoprotein cholesterol (LDL-C), and high-density lipoprotein cholesterol (HDL-C) were analyzed by commercial enzyme assay kits. High non-HDL cholesterol was calculated by subtracting TC from HDL-C.

2.4. Metabolomic analysis

Serum samples from children with obesity before and after weight loss intervention were subjected to liquid chromatography–mass spectrometry (LC–MS) analysis. Take out the serum samples stored at −80 °C and thaw them at room temperature. Transfer 100 μL of the serum sample into a 1.5 mL Eppendorf (EP) tube; Add 400 μL of protein precipitation reagent methanol-acetonitrile (V:V = 2:1, containing L-2-chlorophenylalanine, 2 μg/mL), vortex for 1 min; Ultrasonic extraction in an ice-water bath for 10 min, stand at −40 °C for 30 min; Centrifuge for 10 min (12000 rpm, 4 °C), use a syringe to aspirate 150 μL of the supernatant, filter it through a 0.22 μm organic phase needle filter, and then transfer it to an LC injection vial, store at −80 °C until LC-MS analysis is performed. Quality control samples (QC) are prepared by mixing equal volumes of all sample extracts. All extraction reagents should be precooled at −20 °C before use.

The metabolic profiling of this work was performed by an ACQUITY UPLC-Class system (Waters Corporation, Milford, USA) fitted with a Q Exactive mass spectrometer equipped with a heated electrospray ionization (ESI) source (Thermo Fisher Scientific, Waltham, MA, USA). An ACQUITY UPLC HSS T3 column was used in both positive and negative modes. The details of the mass spectrum parameters are as follows. Spray voltage, 3800 V (+) and 3000 V (−); capillary temperature (°C), 320; aux gas heater temperature (°C), 350; sheath gas flow rate (Arb), 8; S-lens RF level, 50; mass range (*m/z*), 100–1200; full ms resolution, 70000; MS/MS resolution, 17500; NCE/stepped NCE, 10, 20, 40. Progenesis QI V2.3 software (Nonlinear, Dynamics, Newcastle, UK) was used to analyze the original LC–MS data.

The identification of differentially abundant metabolites and bioinformatic analysis were performed using R studio software packages, which include DESeq2, edgeR, and limma packages for statistical analysis to identify differentially abundant metabolites; the ggplot2 package for visualization; the ropls package for multivariate data analysis; and the clusterProfiler package for enrichment analysis. Additionally, the Biostrings and GenomicFeatures packages were used for integration with biological databases. Detailed methods are available in the Supplemental Materials.

2.5. Proteomics analysis

2.5.1. Sample preparation

Twelve serum samples from children with obesity were utilized for proteomics analysis. The process began by diluting 60 μL of serum with Binding Buffer to achieve a 10-fold concentration, resulting in a final volume of 540 μL. The blue cap on the column was removed to eliminate the storage buffer that maintains the resin's hydration. The column was then inverted on a paper towel to ensure complete removal of the storage buffer. Subsequently, the column was placed into an appropriate buffer collection tube. A total of 0.85 mL of Binding Buffer was added to the column, allowing the liquid to pass through the resin bed by gravity flow. The diluted sample was then transferred to the column and allowed to pass through by gravity flow. The flow-through, containing molecules that did not bind to the resin, was collected. The column was then placed into a new buffer collection tube and washed with 600 μL of Binding Buffer to remove any unbound or loosely bound substances. The wash solution was allowed to flow through the resin bed by gravity, and the wash fraction was collected. This washing step was repeated once more with another 600 μL of Binding Buffer to ensure thorough cleaning of the resin and to enhance the specificity of the binding. The combined fraction contained the albumin/IgG-depleted sample. After vacuum freeze-drying, the sample was stored for future use. For resolubilization, 300 μL of SDS lysis buffer was added to the freeze-dried samples. The solution was centrifuged at 12,000 rpm at room temperature for 10 min, and the supernatant was collected. This centrifugation was repeated once more to ensure complete collection of the supernatant. The supernatant represented the total protein solution of the sample. The protein concentration was measured and aliquots were prepared before storage at −80 °C for future use.

The protein concentration of the sample was determined using the BCA (Bicinchoninic Acid) protein assay method. Following the instructions provided with the BCA reagent kit, the coloring reagent was prepared by mixing Buffer A and Buffer B in a volume ratio of 50:1 (v/v). A portion of the protein solution to be tested was diluted with ultrapure water to prevent the concentration from being too high, which could exceed the working range of the standard curve.

A clean 96-well plate was prepared, and a gradient of BSA standard protein solutions was added: 0, 1, 2, 4, 8, 12, 16, 20 μL. Ultrapure water was added to each well to bring the volume up to 20 μL. A diluted protein sample (2 μL) was added to the 96-well plate, with three replicates for each sample, and the volume was adjusted to 20 μL with ultrapure water. A pre-prepared coloring reagent (prepared fresh) was added to each well in a volume of 200 μL, and the plate was incubated at 37 °C for 30 min. Absorbance values were measured using a microplate reader (wavelength 562 nm). The standard curve was calculated based on the known concentrations and absorbance values of the standard protein solutions. The absorbance value of the sample was substituted into the standard curve to determine the protein concentration.

SDS-Polyacrylamide Gel Electrophoresis (SDS-PAGE) was performed on each sample, using 10 μg of protein and a 12 % gel for separation. The separated gel was stained with Coomassie Brilliant Blue using an eStain LG protein staining instrument. The stained gel

was imaged using a fully automated digital gel imaging system.

For trypsin digestion, 50 μg of protein was taken for each sample, diluted to a uniform concentration and volume using the lysis buffer, and DTT was added to the protein solution to a final concentration of 5 mM. The mixture was then incubated at 55 °C for 30 min. After cooling the samples on ice and allowing them to reach room temperature, the appropriate volume of iodacetamide was added to achieve a final concentration of 10 mM. The samples were mixed thoroughly and left in the dark at room temperature for 15 min. Proteins were precipitated by adding an equal volume of acetone, and the samples were placed at −20 °C for 4 h or overnight. The samples were centrifuged at 4 °C at 8000×*g* for 10 min to collect the precipitate, and the acetone was evaporated for 2–3 min. One hundred μL of TEAB (200 mM) was added to resuspend the precipitate, followed by the addition of 1/50 of the sample weight of 1 mg/mL Trypsin-TPCK. The samples were digested overnight at 37 °C, and the digested samples were lyophilized and stored at −80 °C for future use.

2.5.2. Protein digestion and labeling

Based on the measured protein concentration, 50 μg of protein is taken for each sample, and different group samples are diluted and adjusted to the same concentration and volume using lysis buffer. Then, DTT (dithiothreitol) is added to the protein solution to achieve a final concentration of 5 mM, mixed well, and incubated at 55 °C for 30 min. The sample is then cooled on ice until it reaches room temperature (note: the solution should neither feel too cold nor too warm when touched by hand). Next, the appropriate volume of iodacetamide is added to achieve a final concentration of 10 mM, mixed thoroughly, and left in the dark at room temperature for 15 min. Following this, six volumes of acetone are added to the solution to precipitate the proteins, and the mixture is placed at −20 °C for more than 4 h or overnight. The precipitated proteins are collected by centrifugation at 4 °C at 8000×*g* for 10 min. The acetone is then evaporated for 2–3 min. The protein pellet is resuspended in 100 μL of TEAB (200 mM), and 1 mg/mL of Trypsin-TPCK is added at a ratio of 1/50th the weight of the sample. The digestion is carried out overnight at 37 °C. After digestion, the samples are lyophilized (freeze-dried) and stored at −80 °C for future use.

A ProteoExtract™ kit was used to remove the high abundance proteins in serum samples (Millipore, Billerica, MA, United States). For tandem mass tag (TMT) labeling, the lyophilized samples were resuspended, and a TMTsixplex™ kit (Thermo Scientific, Massachusetts, United States) was added to each sample for mixing. The samples were labeled as 126, 127 N, 127C, 128 N, 128C, 129 N, 129C, 130 N, 130C, 131 N, 131C and 132 N.

2.5.3. Chromatography and mass spectrometry

The sample was loaded onto the analytical column, an Acclaim PepMap RSLC (75 μm × 50 cm, RP-C18, Thermo Fisher Scientific), at a flow rate of 300 nL/min for separation. The mobile phases were as follows: Mobile phase A consisted of a mixture of acetonitrile (ACN), water (H2O), and formic acid (FA) in a volume ratio of 99.9:0.1, respectively; mobile phase B was a mixture of acetonitrile, water, and formic acid in a volume ratio of 80:19.9:0.1, respectively. The gradient elution program was set as follows: from 0 to 50 min, the concentration of phase B increased from 2 % to 28 %; from 50 to 60 min, it increased from 28 % to 42 %; from 60 to 65 min, it ramped up to 90 % B; and from 65 to 75 min, it was maintained at 90 % B.

The first-level MS mass resolution was set to 60,000, with the automatic gain control (AGC) target set to 3 × 106, and the maximum injection time was 50 ms. The mass spectrometry scan was configured for a full scan mass-to-charge ratio (m/z) range of 350–1500. MS/MS scans were performed on the 20 most intense peaks. All MS/MS spectra acquisitions were completed using data-dependent high-energy collisional dissociation (HCD) in positive ion mode, with a collision energy set to 32. The MS/MS resolution was set to 45,000, with the AGC target set to 2 × 105, and the ion maximum injection time was 80 ms. The dynamic exclusion time was set to 30 s.

2.5.4. Data search and analysis

The data search sequence file was UniProt-Homo sapiens-9606-2023.2.1.fasta. The search parameters included the following modifications: static modifications were TMT (N-term, K) and Carbamidomethyl (C); dynamic modifications were Oxidation (M) and Acetyl (N-term). The digestion was performed using Trypsin, and the instrument used was a Q Exactive HF. The MS1 tolerance was set at 10 ppm, and the MS2 tolerance was 0.02 Da, with a maximum of 2 missed cleavages.

Proteins were considered reliable if they had a Sequest HT score greater than 0, at least one unique peptide, and no null values in their expression. Proteins with an absolute log2-fold change greater than 0.263 and a p-value less than 0.05 (as determined by a 2-tailed Student's t-test between the Pre group and Post group) were considered differentially expressed proteins (DEPs).

The process of identifying DEPs and conducting bioinformatics analysis was facilitated by the use of various R packages within R Studio. These included the DESeq2, edgeR, and limma packages, which were instrumental in performing statistical analyses to identify DEPs present in varying quantities. For graphical representation, the ggplot2 package was used. The ropls package was employed for a comprehensive analysis of multivariate data, and the clusterProfiler package was essential for performing enrichment analysis. Additionally, the integration with biological databases was achieved seamlessly through the Biostrings and GenomicFeatures packages.

2.6. Statistical analysis

Data are presented as the mean ± standard deviation (SD). Clinical data were compared between the Pre group and Post group using paired Student's *t*-test and the Wilcoxon matched-pairs signed rank test for nonnormally distributed data. The null hypothesis was rejected at $p < 0.05$.

3. Results

3.1. Clinical characteristics of children with obesity before and after weight loss intervention

The clinical characteristics of children with obesity are presented in Fig. 2 (A-I). As previously reported, weight loss intervention significantly decreased BMI (Fig. 2A), waist circumference (Fig. 2B), hip circumference (Fig. 2C) and body fat (Fig. 2D) in the Post group compared with the Pre group. In addition, we analyzed the biochemical indexes of children with obesity before and after weight loss intervention. The results showed that weight loss intervention significantly decreased the levels of TC (Fig. 2E), LDL (Fig. 2I) and high non-HDL cholesterol (Fig. 2H) but not TG (Fig. 2F) and HDL (Fig. 2G) in children with obesity. These results suggest that the weight loss intervention was effective for children with obesity.

3.2. Weight loss intervention significantly changed the proteomic profile in children with obesity

To further explore the proteomic profile of weight loss intervention, TMT-labeled proteome analysis was performed in children with obesity before and after weight loss intervention. There were 4,383 peptides identified from all serum samples of these two groups. Based on this dataset, we identified 548 unique proteins, 43 of which were differentially expressed between the Pre and Post groups in children with obesity ($|\log2\text{fold change}| > 0.263$ and p value < 0.05). Of these, 15 proteins were upregulated and 28 proteins

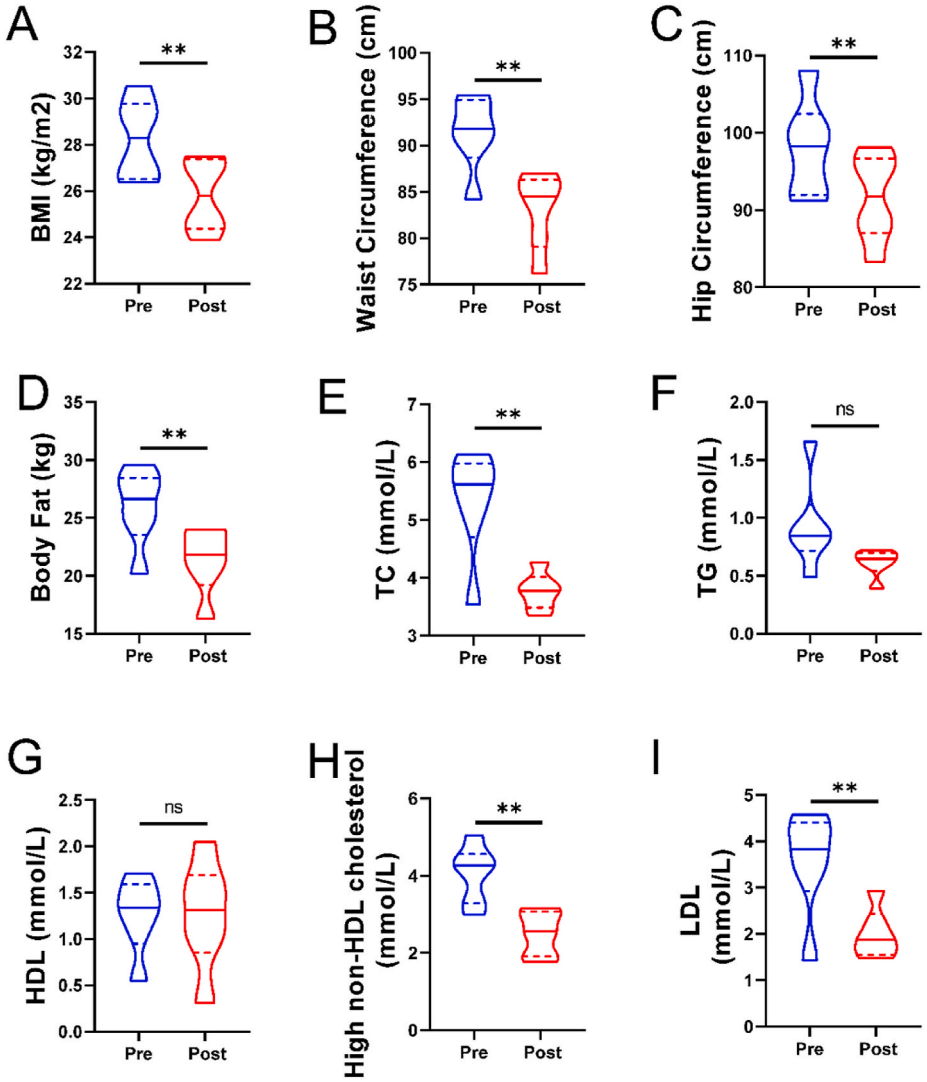

Fig. 2. Weight loss intervention decreased the multiclinical characteristics of obese children. A. Body mass index (BMI); B. Waist circumference; C. Hip circumference; D. Body fat; E. Total cholesterol (TC); F. Total triglyceride (TG); G. High-density lipoprotein cholesterol (HDL); H. High non-HDL; I. Low-density lipoprotein cholesterol (LDL). *$p < 0.05$ between corresponding groups. **$p < 0.01$ between corresponding groups.

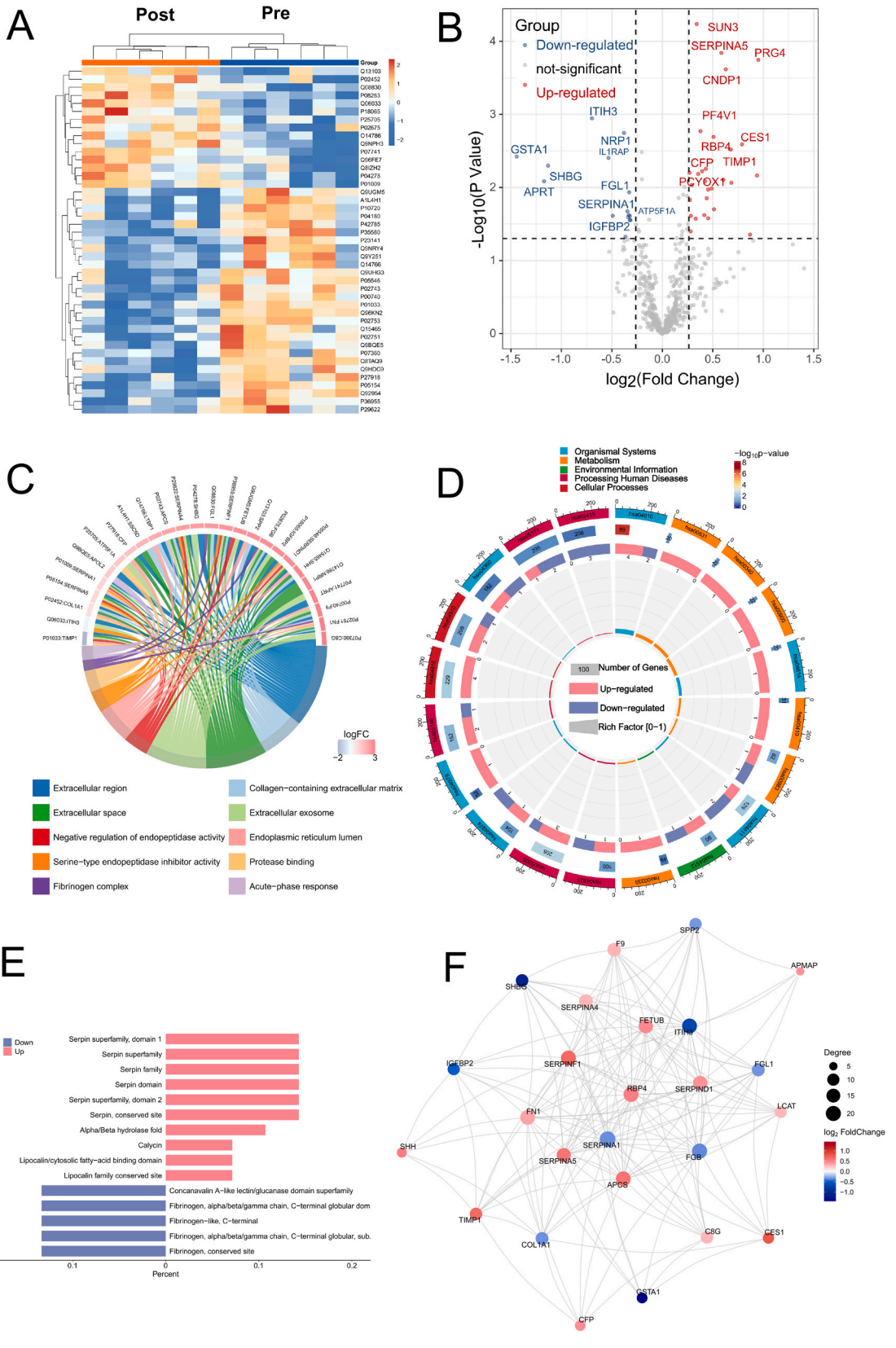

(caption on next page)

Fig. 3. Serum proteomic profile of obese children before and after weight loss intervention. A. Heatmap of 43 differentially expressed proteins between the Pre and Post groups in obese children. B. Volcano plot representing 548 proteins and DEPs. C. GO-based enrichment analysis for DEPs of the Pre and Post groups in obese children. D. KEGG-based enrichment analysis for DEPs of the Pre and Post groups in obese children. E. InterPro-based enrichment analysis for DEPs of the Pre and Post groups in obese children. F. Protein–protein interaction (PPI) analysis network based on the STRING database. Round node size represents the number of connections. Round node color represents DEPs (red represents upregulation, green represents downregulation). (For interpretation of the references to color in this figure legend, the reader is referred to the Web version of this article.)

were downregulated in the Post group compared with the Pre group of children with obesity (Fig. 3A and B).

Next, GO analysis was performed on the 43 differentially expressed proteins to better understand the mechanism involved in weight loss in children with obesity. We chose listhits >2, and the top 10 items with the lowest p values were used to draw the GO enrichment analysis chord diagram. The top ten GO items were extracellular region, extracellular space, negative regulation of endopeptidase activity, serine-type endopeptidase inhibitor activity, fibrinogen complex, collagen-containing extracellular matrix, extracellular exosome, endoplasmic reticulum lumen, protease binding and acute-phase response (Fig. 3C).

As another analysis, we performed KEGG pathway-based analysis on the differentially expressed proteins in children with obesity before and after weight loss intervention. The top 20 significant pathways and their categories, p values, up- and downregulated relationships and richness factors are shown in the KEGG enrichment analysis diagram (Fig. 3D).

In addition, InterPro enrichment analysis was performed based on the InterPro database. The top significantly enriched InterPro terms are shown in Fig. 3E.

Furthermore, a protein–protein interaction (PPI) analysis network based on the STRING database was constructed. In this network, the interaction of different proteins was calculated as the connectivity degree, as shown in Fig. 3F.

3.3. Weight loss intervention significantly changed the metabolomic profile in children with obesity

The metabolomic profile of children with obesity was analyzed as a nontargeted metabolome. Based on the orthogonal projection to latent structures discriminant analysis (OPLS-DA) analysis, we found that there were great differences between the Pre group and the Post group in children with obesity (Fig. 4 A). To confirm that the OPLS-DA model was stable and not accidental, 7-fold cross validation and 200 response permutation tests were performed. The permutation plot confirmed that the OPLS-DA model was stable (Fig. 4 B).

Next, based on the OPLS-DA results, we performed hierarchical clustering on the expression levels of all significant differentially abundant metabolites and the top 50 significant differentially abundant metabolites ranked by variable weight values (VIP) (Fig. 4C). In addition, using volcanoes to visualize p values, VIP values, and fold change values is beneficial for screening differentially abundant metabolites in children with obesity before and after weight loss intervention. The volcano plots showed that 165 metabolites were screened based on VIP >1, $p < 0.05$ and FC > 1 (Fig. 4 D).

In addition, correlation analysis was used to understand the correlation between differentially abundant metabolites. Correlation analysis uses the Pearson correlation coefficient to measure the degree of linear correlation between two metabolites. We performed correlation analysis of the top 20 significantly different metabolites sorted by VIP, which is shown in Fig. 4E.

In addition, to further explore the pathways of weight loss intervention in children with obesity, the KEGG database was used to analyze the differentially abundant metabolites. The top 20 significant pathways and their categories, p values, up- and downregulated relationships and richness factors are shown in the KEGG enrichment analysis diagram (Fig. 4F).

3.4. Integrated-omics analysis based on DEPs and DMs

To directly investigate the relationship between the serum proteomics and metabolomics findings, KGML network analysis was performed. In this analysis, we found that some proteomic adjustments could be reflected by similar changes in the metabolome, and they could be cogrouped in similar or related biochemical pathways to confirm known pathway models. Based on this interaction analysis, 7 KEGG pathways were organically integrated based on the correlation of 7 DEPs and 9 DMs. Histidine metabolism (hsa00340) and glycerophospholipid metabolism (hsa00564) were the high-degree KEGG pathways (Fig. 5A).

In the interaction analysis, we found 7 proteins to be candidate DEPs and 9 metabolites to be candidate DMs. Hierarchical clustering of the 7 candidate DEPs and 9 candidate DMs led to a separation of the Pre group and Post group in children with obesity (Fig. 5B and C).

3.5. Discriminant analyses to distinguish children with obesity before and after weight loss intervention

Based on the candidate DEPs and candidate DMs, we performed OPLS-DA to verify whether these candidates could distinguish children with obesity who had undergone weight loss intervention. Our results showed that 7 candidate DEPs could distinguish children with obesity who had undergone weight loss intervention (Fig. 6A). The permutation test confirmed that the OPLS-DA model was reliable (Fig. 6B). Consistent with these results, we found that 9 candidate DMs could distinguish children with obesity who had undergone weight loss intervention (Fig. 6C), and the OPLS-DA model was also found to be reliable (Fig. 6D).

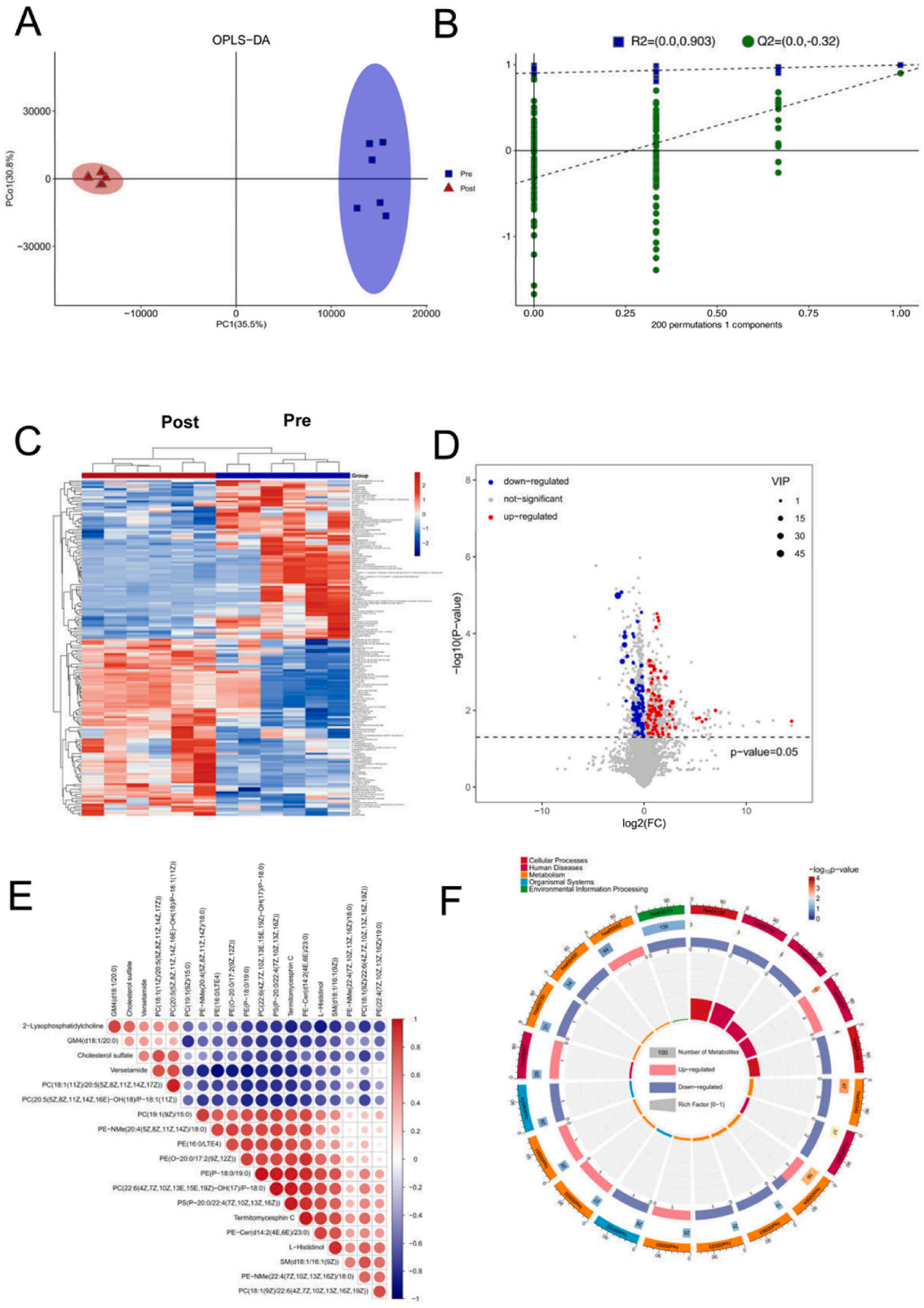

(caption on next page)

Fig. 4. Serum metabolome profile of obese children before and after weight loss intervention. A. Orthogonal projection to latent structures discriminant analysis (OPLS-DA) plot; B. Permutation plot; C. Heatmap of differentially expressed metabolites. D. Volcano plot representing candidate metabolites. Red represents upregulated metabolites ($p < 0.05$, VIP >1 and FC > 1), and blue represents downregulated metabolites ($p < 0.05$, VIP >1 and FC > 1). E. Correlation heatmap for the top 20 differentially expressed metabolites (based on the VIP). Red indicates a positive correlation, blue indicates a negative correlation, and the larger the round node size is, the greater the correlation coefficient between the two metabolites. F. KEGG-based enrichment analysis for differentially expressed metabolites of the Pre and Post groups in obese children. (For interpretation of the references to color in this figure legend, the reader is referred to the Web version of this article.)

3.6. Correlation analysis between candidate DEPs, DMs and clinical characteristics of children with obesity before and after weight loss intervention

To investigate whether clinical characteristics, including BMI, body fat percentage, hip circumference, waist circumference, HDL, LDL, TC, TG, and high non-HDL cholesterol, were mirrored in the candidate DEPs, DM correlation analysis was performed between them. Remarkably, 4 candidate DEPs (glutathione S-transferase A1 (GSTA1), lysosomal Pro-X carboxypeptidase (PRCP), myosin-10 (MYH10), and carnosine dipeptidase 1 (CNDP1)) and 2 DMs (uric acid and 2-lysophosphatidylcholine) were significantly correlated with BMI (Fig. 7A). In this analysis, we found that most classical clinical parameters were significantly correlated with DEPs and DMs, except HDL (Fig. 7B–I). In addition, most DEPs and DMs were significantly associated with high non-HDL cholesterol. All the results suggested that the clinical parameters were mirrored in the serum candidate DEPs and DMs.

4. Discussion

In the present study, we integrated the proteomics and metabolomics profiles of children with obesity before and after weight loss intervention for the first time. We found that weight loss interventions significantly decreased BMI, waist circumference, hip circumference, body fat, TC, high non-HDL cholesterol and LDL. In addition, we found that 4 weeks of weight loss intervention significantly changed the proteomic and metabolomic profiles in children with obesity. We also found that 7 KEGG pathways were organically integrated based on the correlation of 7 DEPs and 9 DMs in children with obesity after weight loss intervention. Furthermore, we demonstrated that 7 candidate DEPs and 9 candidate DMs could distinguish children with obesity who had undergone weight loss intervention. Together, these data suggest that 4 weeks of lifestyle intervention could significantly decrease BMI by modulating proteomic and metabolomic profiles.

Lifestyle intervention is the first recommended method for weight loss in children with obesity. In the present study, we found that 4 weeks of lifestyle intervention significantly decreased BMI, waist circumference, hip circumference, body fat, TC, high non-HDL cholesterol and LDL. These results are consistent with previous studies [13,14].

To explore the mechanism involved in the effects of lifestyle intervention in children with obesity, proteomics and metabolomics analyses were performed. The proteomics approach has been widely used in obesity studies [15]. Similar to previous reports [16], our proteomics analysis revealed that lifestyle intervention significantly changes the proteomic profile in children with obesity. In addition, several previous studies demonstrated that metabolites change after weight loss interventions [8,17]. For example, one study showed that obese and overweight individuals showed unique blood metabolite signatures after energy-restricted diet weight loss intervention for 12 weeks [17]. In addition, our previous study showed that weight loss intervention (exercise combined with dietary control) significantly improved body composition and plasma metabolites [13]. Consistent with these results, we found that lifestyle intervention significantly changes the metabolomics profiles of children with obesity.

To directly investigate the underlying mechanisms of serum proteomics and metabolomics, KGML network analysis was performed. Seven KEGG pathways were organically integrated based on the correlation of 7 DEPs and 9 DMs. Histidine metabolism was found to be one of the high-degree KEGG pathways in this analysis and may play an important role in the prevention of obesity [18]. Serum histidine levels are lower in obese individuals [19], and histidine supplementation could significantly decrease inflammation, oxidative stress, BMI, IR and body fat mass in obese individuals with metabolic syndrome [20]. In addition, we found that glycerophospholipid metabolism was another high-degree KEGG pathway in this analysis. Glycerophospholipid metabolism plays a key role in cellular membrane dynamics and lipid balance [21]. In addition, glycerophospholipid metabolism has been analyzed in many metabolic disorders, such as IR and obesity [22]. Consistent with these reports, we found that weight loss intervention significantly changed the glycerophospholipid metabolism pathway in children with obesity.

Based on the interaction analysis, we found 7 proteins as candidate DEPs and 9 metabolites as candidate DMs. Many of these candidate DEPs and DMs could distinguish whether children with obesity had undergone weight loss intervention by OPLS-DA and readily explain weight loss biology and physiology. For instance, the levels of lecithin cholesterol acyltransferase (LCAT), which is a crucial enzyme for HDL metabolism [23,24], are significantly increased, mirroring IR and diet-induced obesity [25]. The levels of MYH10 are increased in obese pregnant mice [26], and its interaction with insulin-dependent glucose transporter 4 (GLUT4) regulates adipocyte function and adipogenesis [27]. The findings of these studies are conceptually consistent with our results that the levels of MYH10 were significantly decreased in children with obesity who had undergone weight loss intervention and may play an important role in weight loss. Uric acid has been associated with obesity, metabolic syndrome and prehypertension [28–30], and our results found that uric acid levels significantly decreased in response to weight loss intervention in children with obesity.

Interestingly, we found that some candidate DEPs and DMs were significantly correlated with clinical parameters. For instance, GSTA1 plays a crucial role in protecting tissue from oxidative stress [31,32], and we found that GSTA1 was significantly negatively correlated with BMI. CNDP1 is involved in pathological and physiological processes [33–35] and is associated with weight loss and

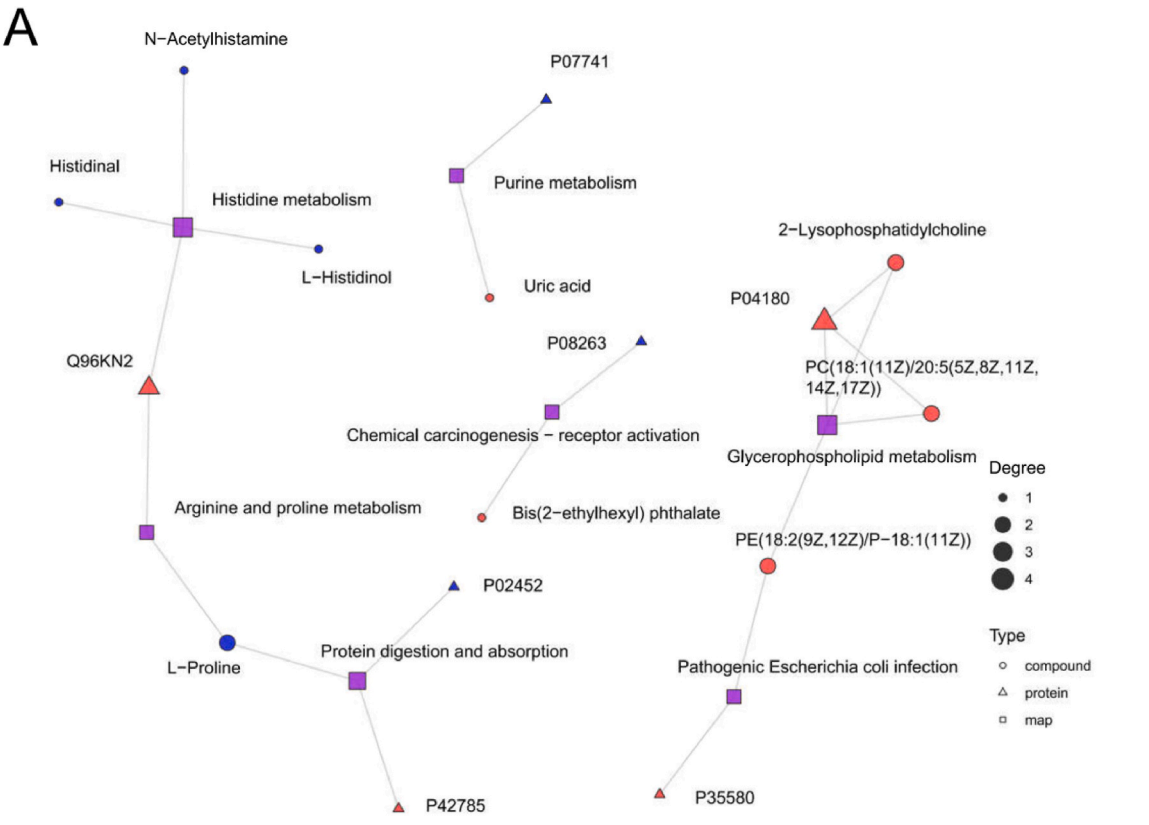

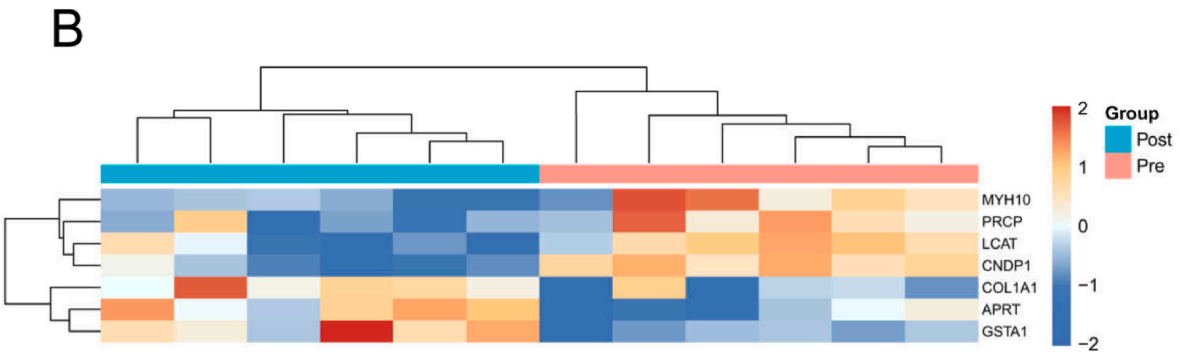

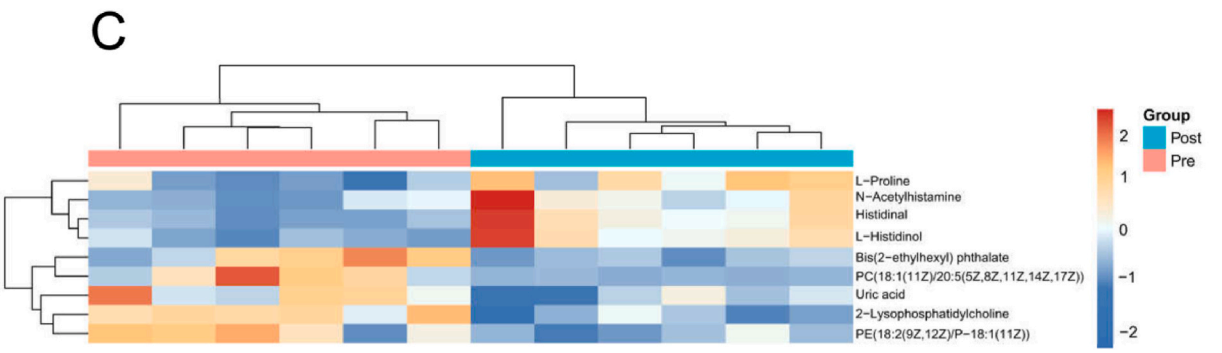

(caption on next page)

Fig. 5. Integrated proteomics and metabonomics analysis of obese children before and after weight loss intervention. A. KGML network analysis of proteomics and metabonomics profiles. KGML is a sublibrary of the KEGG database that includes both the relationships between graphical objects in the KEGG pathway and the information of homologous genes in the KEGG GENES database, which provides information on the network relationship between proteins and metabolites. The squares represent pathways, triangles represent proteins, and circles represent metabolites. Red represents upregulated proteins or metabolites, while blue represents downregulated proteins or metabolites. Degree represents the number of connections between them. B. Clustering heatmap of 7 differentially expressed proteins in obese children before and after weight loss interventions. C. Clustering heatmap of 9 differentially expressed metabolites in obese children before and after weight loss interventions. (For interpretation of the references to color in this figure legend, the reader is referred to the Web version of this article.)

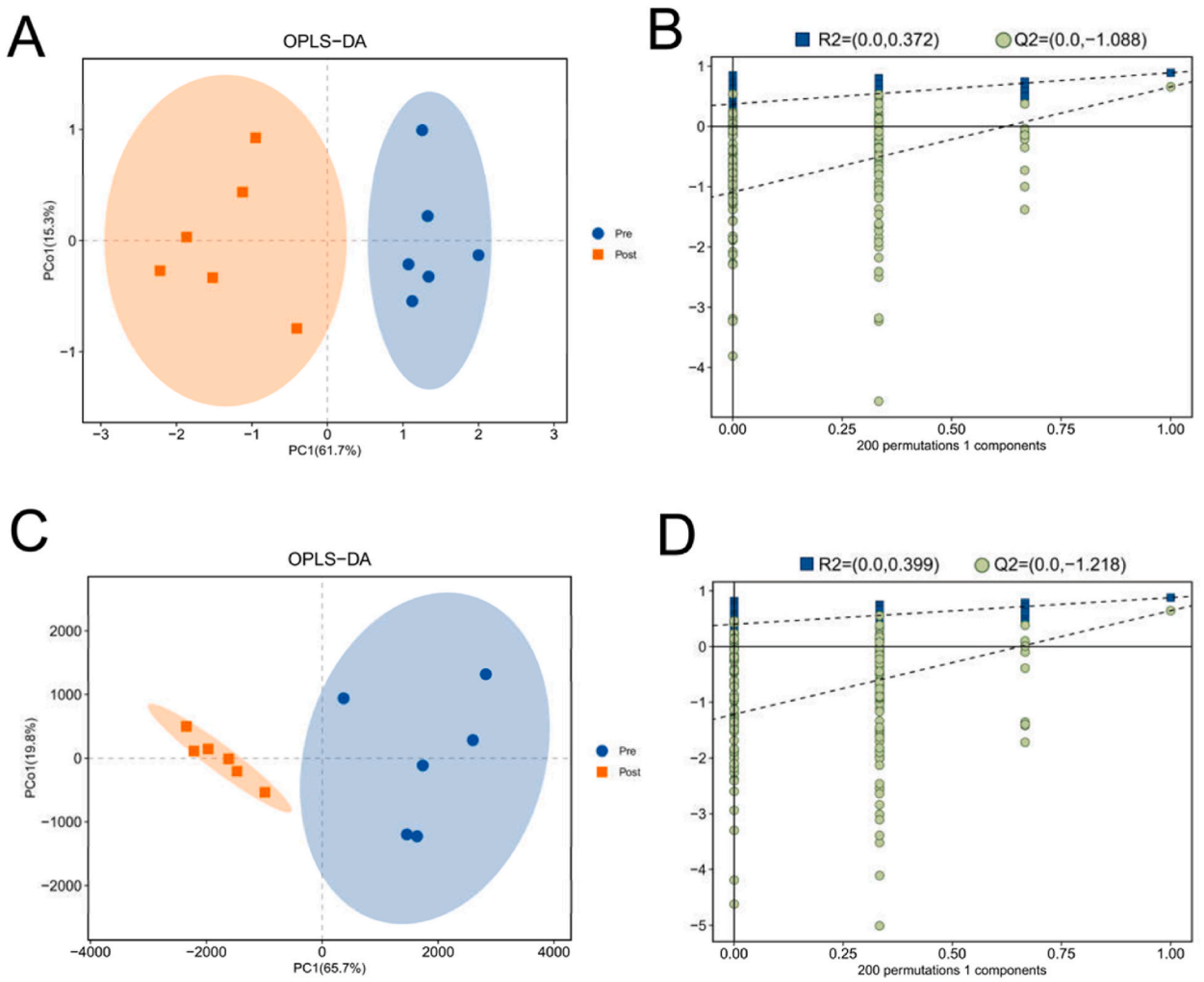

Fig. 6. Discriminant analyses to distinguish obese children before and after weight loss intervention. A. OPLS-DA plot of 7 candidate proteins. B. Permutation plot of 7 candidate proteins. C. OPLS-DA plot of 9 candidate metabolites. D. Permutation plot of 9 candidate metabolites.

cancer progression [36]. Consistent with these reports, we found that CNDP1 was significantly positively correlated with BMI. 2-Lysophosphatidylcholines (1-acyl-glycero-3-phosphocholines) are involved in glucose homeostasis [37], which was positively correlated with BMI in our study. However, correction analysis was performed between other candidate DEPs, DMs and clinical parameters. These results suggested that some clinical parameters could be mirrored in the serum DEPs and DMs.

There are some limitations to our study. First, serum samples were used for analysis in this study, which may have small differences between plasma samples. However, many studies have used serum samples to research the proteome and metabolome. Second, the sample size was small in this weight loss intervention study. Another possible drawback of this study is that although we found some DEPs and DMs, their specific roles in children's weight loss need to be further investigated. In addition, whether these proteins and metabolites can be targeted for clinical treatment should be further investigated.

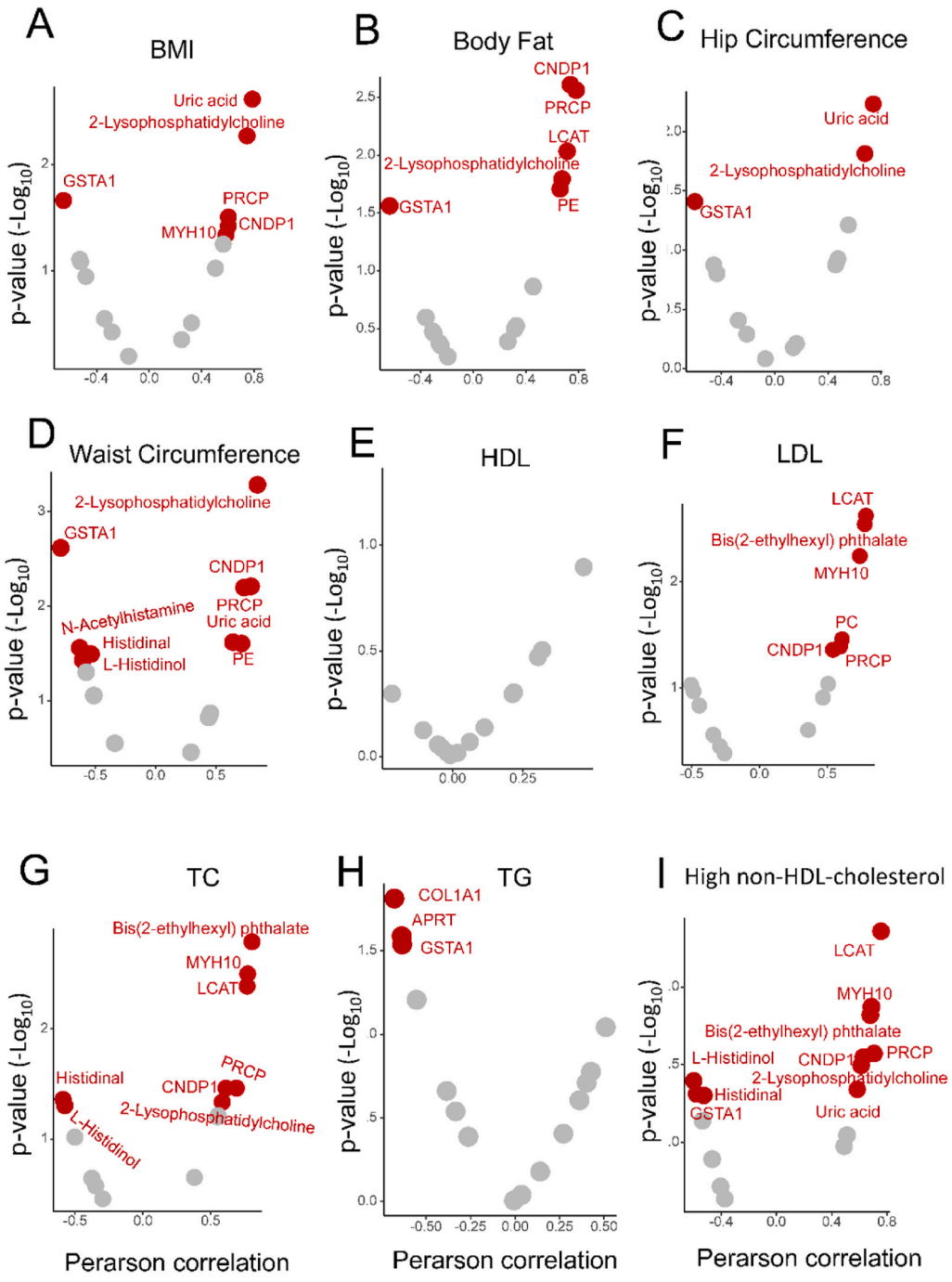

Fig. 7. The correction analysis between candidate DEPs, DMs and clinical characteristics of obese children before and after weight loss intervention. A. Correlation of BMI with DEPs and DMs. B. Correlation of body fat with DEPs and DMs. C. Correlation of hip circumference with DEPs and DMs. D. Correlation of waist circumference with DEPs and DMs. E. Correlation of HDL with DEPs and DMs. F. Correlation of LDL with DEPs and DMs. G. Correlation of TC with DEPs and DMs. H. Correlation of TG with DEPs and DMs. I. Correlation of high non-HDL-cholesterol with DEPs and DMs.

5. Conclusions

Our study provides valuable proteomic and metabolomic data resources for better understanding weight loss-associated responses in children with obesity. In addition, we analyzed the number of significantly differentially expressed proteins and metabolites, shed new light on weight loss pathogenesis in children with obesity, and added to the list of potential therapeutic agents for obese and overweight children.

Availability of data and materials

The data reported in this paper have been deposited in the OMIX, China National Center for Bioinformation/Beijing Institute of Genomics, Chinese Academy of Sciences (https://ngdc.cncb.ac.cn/omix: accession no. OMIX005304 and OMIX005305).

Funding

This work was supported by the (Ministry of Education in China) Project of Humanities and Social Sciences (No. 22YJC890014), Guangdong Province Universities and Colleges Pearl River Scholar Funded Scheme (2019).

CRediT authorship contribution statement

Xiaoguang Liu: Writing – review & editing, Writing – original draft, Visualization, Validation, Supervision, Software, Resources, Project administration, Methodology, Investigation, Funding acquisition, Formal analysis, Data curation, Conceptualization.**Huiguo Wang:** Writing – review & editing, Conceptualization. **Lin Zhu:** Writing – review & editing, Investigation, Funding acquisition, Conceptualization.

Declaration of competing interest

The authors declare that they have no known competing financial interests or personal relationships that could have appeared to influence the work reported in this paper.

Acknowledgements

We gratefully acknowledge the valuable contributions of THE BIGGEST LOSER in data collection.

Appendix A. Supplementary data

Supplementary data to this article can be found online at https://doi.org/10.1016/j.heliyon.2024.e31917.

References

[1] P.G. McPhee, S. Singh, K.M. Morrison, Childhood obesity and cardiovascular disease risk: working toward solutions, Can. J. Cardiol. 36 (2020) 1352–1361, https://doi.org/10.1016/j.cjca.2020.06.020.
[2] Obesity and overweight, (n.d.). https://www.who.int/news-room/fact-sheets/detail/obesity-and-overweight (accessed August 2, 2023).
[3] M. Heitkamp, M. Siegrist, S. Molnos, S. Brandmaier, S. Wahl, H. Langhof, H. Grallert, M. Halle, Obesity genes and weight loss during lifestyle intervention in children with obesity, JAMA Pediatr. 175 (2021) e205142, https://doi.org/10.1001/jamapediatrics.2020.5142.
[4] A.M. Mahmoud, An overview of epigenetics in obesity: the role of lifestyle and therapeutic interventions, Int. J. Mol. Sci. 23 (2022) 1341, https://doi.org/10.3390/ijms23031341.
[5] B.J. Ryan, M.W. Schleh, C. Ahn, A.C. Ludzki, J.B. Gillen, P. Varshney, D.W. Van Pelt, L.M. Pitchford, T.L. Chenevert, R.A. Gioscia-Ryan, S.M. Howton, T. Rode, S. L. Hummel, C.F. Burant, J.P. Little, J.F. Horowitz, Moderate-intensity exercise and high-intensity interval training affect insulin sensitivity similarly in obese adults, J. Clin. Endocrinol. Metab. 105 (2020) e2941–e2959.
[6] L. Stoner, D. Rowlands, A. Morrison, D. Credeur, M. Hamlin, K. Gaffney, D. Lambrick, A. Matheson, Efficacy of exercise intervention for weight loss in overweight and obese adolescents: meta-analysis and implications, Sports Med. 46 (2016) 1737–1751, https://doi.org/10.1007/s40279-016-0537-6.
[7] E.T. Cirulli, L. Guo, C. Leon Swisher, N. Shah, L. Huang, L.A. Napier, E.F. Kirkness, T.D. Spector, C.T. Caskey, B. Thorens, J.C. Venter, A. Telenti, Profound perturbation of the metabolome in obesity is associated with health risk, Cell Metabol. 29 (2019) 488–500.e2, https://doi.org/10.1016/j.cmet.2018.09.022.
[8] M.-J. Sohn, W. Chae, J.-S. Ko, J.-Y. Cho, J.-E. Kim, J.-Y. Choi, H.-B. Jang, H.-J. Lee, S.-I. Park, K.-H. Park, P.J. van der Spek, J.-S. Moon, Metabolomic signatures for the effects of weight loss interventions on severe obesity in children and adolescents, Metabolites 12 (2022) 27, https://doi.org/10.3390/metabo12010027.
[9] J. Carayol, C. Chabert, A. Di Cara, C. Armenise, G. Lefebvre, D. Langin, N. Viguerie, S. Metairon, W.H.M. Saris, A. Astrup, P. Descombes, A. Valsesia, J. Hager, Protein quantitative trait locus study in obesity during weight-loss identifies a leptin regulator, Nat. Commun. 8 (2017) 2084, https://doi.org/10.1038/s41467-017-02182-z.
[10] A.P. Doumatey, J. Zhou, M. Zhou, D. Prieto, C.N. Rotimi, A. Adeyemo, Proinflammatory and lipid biomarkers mediate metabolically healthy obesity: a proteomics study, Obesity (Silver Spring, Md 24 (2016) 1257–1265, https://doi.org/10.1002/oby.21482.
[11] E. López-Villar, G.Á. Martos-Moreno, J.A. Chowen, S. Okada, J.J. Kopchick, J. Argente, A proteomic approach to obesity and type 2 diabetes, J. Cell Mol. Med. 19 (2015) 1455–1470, https://doi.org/10.1111/jcmm.12600.
[12] J. Shao, T. Pan, J. Wang, T. Tang, Y. Li, X. Jia, S. Lai, Integrated proteomics and metabolomics analysis of perirenal adipose tissue in obese rabbits treated with a restricted diet, Biology 10 (2021) 321, https://doi.org/10.3390/biology10040321.
[13] J. Liu, L. Zhu, J. Liao, X. Liu, Effects of extreme weight loss on cardiometabolic health in children with metabolic syndrome: a metabolomic study, Front. Physiol. 12 (2021) 731762, https://doi.org/10.3389/fphys.2021.731762.
[14] H. Oude Luttikhuis, L. Baur, H. Jansen, V.A. Shrewsbury, C. O'Malley, R.P. Stolk, C.D. Summerbell, WITHDRAWN: interventions for treating obesity in children, Cochrane Db. Syst. Rev. 3 (2019) CD001872, https://doi.org/10.1002/14651858.CD001872.pub3.
[15] E. López-Villar, G.Á. Martos-Moreno, J.A. Chowen, S. Okada, J.J. Kopchick, J. Argente, A proteomic approach to obesity and type 2 diabetes, J. Cell Mol. Med. 19 (2015) 1455–1470, https://doi.org/10.1111/jcmm.12600.
[16] P.E. Geyer, N.J. Wewer Albrechtsen, S. Tyanova, N. Grassl, E.W. Iepsen, J. Lundgren, S. Madsbad, J.J. Holst, S.S. Torekov, M. Mann, Proteomics reveals the effects of sustained weight loss on the human plasma proteome, Mol. Syst. Biol. 12 (2016) 901, https://doi.org/10.15252/msb.20167357.
[17] B.D. Piccolo, N.L. Keim, O. Fiehn, S.H. Adams, M.D. Van Loan, J.W. Newman, Habitual physical activity and plasma metabolomic patterns distinguish individuals with low vs. high weight loss during controlled energy restriction, J. Nutr. 145 (2015) 681–690, https://doi.org/10.3945/jn.114.201574.

[18] J.J. DiNicolantonio, M.F. McCarty, J.H. Okeefe, Role of dietary histidine in the prevention of obesity and metabolic syndrome, Open Heart 5 (2018) e000676, https://doi.org/10.1136/openhrt-2017-000676.
[19] Y.-C. Niu, R.-N. Feng, Y. Hou, K. Li, Z. Kang, J. Wang, C.-H. Sun, Y. Li, Histidine and arginine are associated with inflammation and oxidative stress in obese women, Br. J. Nutr. 108 (2012) 57–61, https://doi.org/10.1017/S0007114511005289.
[20] R.N. Feng, Y.C. Niu, X.W. Sun, Q. Li, C. Zhao, C. Wang, F.C. Guo, C.H. Sun, Y. Li, Histidine supplementation improves insulin resistance through suppressed inflammation in obese women with the metabolic syndrome: a randomised controlled trial, Diabetologia 56 (2013) 985–994, https://doi.org/10.1007/s00125-013-2839-7.
[21] S. Rodriguez-Cuenca, V. Pellegrinelli, M. Campbell, M. Oresic, A. Vidal-Puig, Sphingolipids and glycerophospholipids – the "ying and yang" of lipotoxicity in metabolic diseases, Prog. Lipid Res. 66 (2017) 14–29, https://doi.org/10.1016/j.plipres.2017.01.002.
[22] D. Liu, J. Wang, H. Zeng, F. Zhou, B. Wen, X. Zhang, Y. Luo, W. Wu, J. Huang, Z. Liu, The metabolic regulation of fuzhuan brick tea in high-fat diet-induced obese mice and the potential contribution of gut microbiota, Food Funct. 13 (2022) 356–374, https://doi.org/10.1039/D1FO02181H.
[23] J.T. Stadler, S. Lackner, S. Mörkl, A. Trakaki, H. Scharnagl, A. Borenich, W. Wonisch, H. Mangge, S. Zelzer, N. Meier-Allard, S.J. Holasek, G. Marsche, Obesity affects HDL metabolism, composition and subclass distribution, Biomedicines 9 (2021) 242, https://doi.org/10.3390/biomedicines9030242.
[24] K. Yang, J. Wang, H. Xiang, P. Ding, T. Wu, G. Ji, LCAT- targeted therapies: progress, failures and future, Biomedicine & Pharmacotherapy = Biomedecine & Pharmacotherapie 147 (2022) 112677, https://doi.org/10.1016/j.biopha.2022.112677.
[25] L. Li, M.A. Hossain, S. Sadat, L. Hager, L. Liu, L. Tam, S. Schroer, L. Huogen, I.G. Fantus, P.W. Connelly, M. Woo, D.S. Ng, Lecithin cholesterol acyltransferase null mice are protected from diet-induced obesity and insulin resistance in a gender-specific manner through multiple pathways, J. Biol. Chem. 286 (2011) 17809–17820, https://doi.org/10.1074/jbc.M110.180893.
[26] K. Schmitz, E.-M. Turnwald, T. Kretschmer, R. Janoschek, I. Bae-Gartz, K. Voßbrecher, M.D. Kammerer, A. Köninger, A. Gellhaus, M. Handwerk, M. Wohlfarth, D. Gründemann, E. Hucklenbruch-Rother, J. Dötsch, S. Appel, Metformin prevents key mechanisms of obesity-related complications in visceral white adipose tissue of obese pregnant mice, Nutrients 14 (2022) 2288, https://doi.org/10.3390/nu14112288.
[27] N. Kislev, L. Mor-Yossef Moldovan, R. Barak, M. Egozi, D. Benayahu, MYH10 governs adipocyte function and adipogenesis through its interaction with GLUT4, Int. J. Mol. Sci. 23 (2022) 2367, https://doi.org/10.3390/ijms23042367.
[28] S. Anjos, E. Feiteira, F. Cerveira, T. Melo, A. Reboredo, S. Colombo, R. Dantas, E. Costa, A. Moreira, S. Santos, A. Campos, R. Ferreira, P. Domingues, M.R. M. Domingues, Lipidomics reveals similar changes in serum phospholipid signatures of overweight and obese pediatric subjects, J. Proteome Res. 18 (2019) 3174–3183, https://doi.org/10.1021/acs.jproteome.9b00249.
[29] S. Liu, Y. Wang, H. Liu, T. Xu, M.-J. Wang, J. Lu, Y. Guo, W. Chen, M. Ke, G. Zhou, Y. Lu, P. Chen, W. Zhou, Serum lipidomics reveals distinct metabolic profiles for asymptomatic hyperuricemic and gout patients, Rheumatology 61 (2022) 2644–2651, https://doi.org/10.1093/rheumatology/keab743.
[30] B. Soletsky, D.I. Feig, Uric acid reduction rectifies prehypertension in obese adolescents, Hypertension 60 (2012) 1148–1156, https://doi.org/10.1161/HYPERTENSIONAHA.112.196980.
[31] M.T.M. Raijmakers, H.M.J. Roelofs, E.A.P. Steegers, R. égine P.M. Steegers-Theunissen, T.P.J. Mulder, M.F.C.M. Knapen, W.Y. Wong, W.H.M. Peters, Glutathione and glutathione S-transferases a1-1 and p1-1 in seminal plasma may play a role in protecting against oxidative damage to spermatozoa, Fertil. Steril. 79 (2003) 169–172, https://doi.org/10.1016/S0015-0282(02)04404-7.
[32] S. Suvakov, T. Damjanovic, A. Stefanovic, T. Pekmezovic, A. Savic-Radojevic, M. Pljesa-Ercegovac, M. Matic, T. Djukic, V. Coric, J. Jakovljevic, J. Ivanisevic, S. Pljesa, Z. Jelic-Ivanovic, J. Mimic-Oka, N. Dimkovic, T. Simic, Glutathione S-transferase a1, m1, p1 and t1 null or low-activity genotypes are associated with enhanced oxidative damage among haemodialysis patients, Nephrol. Dial. Transplant. 28 (2013) 202–212, https://doi.org/10.1093/ndt/gfs369.
[33] B. Gualano, I. Everaert, S. Stegen, G.G. Artioli, Y. Taes, H. Roschel, E. Achten, M.C. Otaduy, A.H.L. Junior, R. Harris, W. Derave, Reduced muscle carnosine content in type 2, but not in type 1 diabetic patients, Amino Acids 43 (2012) 21–24, https://doi.org/10.1007/s00726-011-1165-y.
[34] U. Qundos, H. Johannesson, C. Fredolini, G. O'Hurley, R. Branca, M. Uhlén, F. Wiklund, A. Bjartell, P. Nilsson, J.M. Schwenk, Analysis of plasma from prostate cancer patients links decreased carnosine dipeptidase 1 levels to lymph node metastasis, Transl, Proteomics 2 (2014) 14–24, https://doi.org/10.1016/j.trprot.2013.12.001.
[35] H.A. Chakkera, R.L. Hanson, S. Kobes, M.P. Millis, R.G. Nelson, W.C. Knowler, J.K. DiStefano, Association of variants in the carnosine peptidase 1 gene (CNDP1) with diabetic nephropathy in American Indians, Mol. Genet. Metabol. 103 (2011) 185–190, https://doi.org/10.1016/j.ymgme.2011.02.010.
[36] P. Arner, F. Henjes, J.M. Schwenk, S. Darmanis, I. Dahlman, B.-M. Ireskjö, P. Naredi, T. Agustsson, K. Lundholm, P. Nilsson, M. Rydén, Circulating carnosine dipeptidase 1 associates with weight loss and poor prognosis in gastrointestinal cancer, PLoS One 10 (2015) e0123566, https://doi.org/10.1371/journal.pone.0123566.
[37] A. Drzazga, A. Sowińska, A. Krzemińska, A. Okruszek, P. Paneth, M. Koziołkiewicz, E. Gendaszewska-Darmach, 2-OMe-lysophosphatidylcholine analogues are GPR119 ligands and activate insulin secretion from βTC-3 pancreatic cells: evaluation of structure-dependent biological activity, Biochim. Biophys. Acta Mol. Cell Biol. Lipids 1863 (2018) 91–103, https://doi.org/10.1016/j.bbalip.2017.10.004.

List of abbreviations

TC: total cholesterol
HDL: high-density lipoprotein cholesterol
TG: triglyceride
LDL: low-density lipoprotein cholesterol
DEPs: differentially expressed proteins
DMs: differentially expressed metabolites
WHO: World Health Organization
BMI: body mass index
PPI: protein–protein interaction
VIP: variable weight values
GSTA1: glutathione S-transferase A1
PRCP: lysosomal Pro-X carboxypeptidase
MYH10: myosin-10
CNDP1: carnosine dipeptidase 1